Cell population migration cycle and response to environmental pH in *Bacillus subtilis*

Sohei Tasaki[1*], Madoka Nakayama[2], Izumi Takagi[3,4], Jun-ichi Wakita[5], Wataru Shoji[6]

[1]Department of Mathematics, Faculty of Science, Hokkaido University, Kita-10, Nishi-8, Kita-ku, Sapporo, Hokkaido 060-0810, Japan

[2]Department of General Engineering, Sendai National College of Technology, 48 Nodayama, Medeshima-Shiote, Natori, Miyagi 981-1239, Japan

[3]Mathematical Institute, Tohoku University, 6-3 Aramaki-aza-Aoba, Aoba-ku, Sendai, Miyagi 980-8579, Japan

[4]Institute for Mathematical Sciences, Renmin University of China, No 59 Zhongguancun Street, Haidian District, Beijing 100872, China

[5]Department of Physics, Chuo University, Kasuga 1-13-27, Bunkyo-ku, Tokyo 112-8551, Japan

[6]Frontier Research Institute for Interdisciplinary Sciences (FRIS), Tohoku University, 6-3 Aramaki-aza-Aoba, Aoba-ku, Sendai, Miyagi 980-8579, Japan

[*]Corresponding Author: tasaki@math.sci.hokudai.ac.jp

Running title: Cell population migration cycle in *B. subtilis*

Abstract

Microbial populations are ubiquitous and some form a robust, multicellular structure called biofilm that protects the cells from environmental damage. The dispersion cycle is critical for controlling the population of important target microbes (both pathogenic and beneficial). Here, we show that the hysteresis of *Bacillus subtilis* cell-type regulation with respect to auto-inducing signal strength triggers the migration cycle of the cell population. We investigate migration cycle and its dependence on environmental conditions by quantitative analysis of cyclically expanding, concentric circular colonies. Next, we construct an input/output model that controls cell types in response to environmental conditions and signal density. On the basis of this model, we propose a migration cycle model for cell populations. The proposed model will widely predict biofilm-related phenomena and provide the basis for the description of highly self-regulating multicellular systems.

Introduction

Microbial populations form colonies and they often exist stably in a robust system called biofilm[1-8]. The structural robustness of biofilms makes it difficult to kill disease-related microorganisms[9-11]. In addition, myriads of useful microorganisms are also being discovered, so controlling the population of target microorganisms is an urgent issue[12-14]. The process of biofilm formation is as follows: (i) bacteria attach themselves to suitable surfaces available in the environment; (ii) they proliferate while secreting extracellular polymeric substances (EPS) to form a biofilm; (iii) when the colony becomes large and the cell density increases, the outer wall is destroyed and mobile cells are released. These released cells wander around in search for a new environment suitable for growth. When they identify an environment that satisfies their growth requirements, they become non-migrating cells and colonize that environment. To summarize, these cells return to the first phase of biofilm formation as described in (i) above. This cycle of repeating a series of phases is called the life cycle of a bacterial biofilm. The concept of life cycle was originally used for individual organisms, whereas in a biofilm, it is used for

a group of cells. Therefore, it involves multilevel interactions, such as information transfer within and between groups. However, the details of the biofilm life cycle generation mechanism are not well understood.

A phenomenon similar to the life cycle of biofilms is the formation of concentric circular colonies that embody the migration cycle of bacterial cell populations. (Fig. 1). *Proteus mirabilis*[15-18] and *Bacillus subtilis*[18-23] are known to form concentric colonies. During their formation, the dominant cell population for colony growth switches periodically between migrating and non-migrating states. In *B. subtilis*, the migrating cell population consists of motile cells, which can swim by bundling and rotating multiple flagella[24]. Particularly, two-dimensional collective movement, called swarming, by motile cells plays a central role in rapid space expansion during the migration phase of the life cycle[25-27]. There are three possible factors that cause the cell population to become non-migrating—without swarming motility—: (i) switching to an immotile cell type; (ii) cessation of hyperflagellation; and (iii) insufficient concentration of surface-wetting molecules, such as surfactin. In the case of this *B. subtilis* concentric colony, the non-migrating cell population is in the form of matrix-producer-like chains of proliferating cell populations, and the cells do not move at all[21]. Therefore, the major mechanism underlying the stoppage of swarming involves the predominance of immotile cell types, most of which are matrix producers. Although the regulation of surface-wetting molecule secretion and hyperflagellation should also be involved in the stabilization of the cycle, we will consider this subject in a future research. Thus, here, we focus on cell type switching. A matrix producer does not move, and it proliferates while producing extracellular matrices[28]. The number of cells increases because of cell division, but in this phase, intercellular adhesion is strong and separation is rare[29, 30]. Therefore, the cell group looks like a thread that continues to grow, and its growth mode is called chaining or bundling. The colony not only expands two dimensionally but also increases in thickness (grows in the direction perpendicular to the medium plane). Cells called surfactin producers[31, 32] are known to coexist to assist the slow two-dimensional expansion in this case, improving sliding mobility

71 on the medium surface[33], although it is far behind the expansion speed during the migration phase. In
72 this way, the repetition of the two phases, the migration phase in which cells rapidly spread on the
73 surface of the medium and the growth phase in which migration stops and the thickness increases,
74 exactly represents the migration cycle of *B. subtilis* concentric colonies.

75 Although the process of concentric colony formation is known in this way, the detailed mechanism
76 remains unclear. This is because of the lack of information on environment-dependent control patterns
77 between different cell types, mobile and non-mobile. By focusing on *B. subtilis*, various mutually
78 exclusive cell types have been discovered [24]. The balance between motile cells and matrix producers
79 is particularly important for the migration cycle of the cell population. The genes related to each of
80 these two types are mutually exclusive because of self-activation and mutual repression. When this
81 mutual exclusivity becomes stronger, hysteresis occurs in cell-type regulation and a migration cycle is
82 induced in the cell population, resulting in the formation of concentric circular colonies. Specifically,
83 whether or not concentric colonies are formed depends on the presence or absence of hysteresis during
84 cell-type control of the cell population and on environmental conditions. Investigating the conditions
85 for forming concentric colonies is essential for understanding the life cycle generation mechanism of
86 cell populations.

87 However, the conditions for forming concentric colonies of *B. subtilis* have not yet been clearly
88 determined, although the need for agar concentrations of about 0.7% in solid medium and high nutrient
89 conditions is known[19, 21]. Particularly, the agar concentration is required to be in the range of 0.65–
90 0.75%. In addition, the incubation temperature is preferably 25–35°C, which is lower than the usual
91 35–37°C[19], and long-term pre-drying of the medium surface is desirable[21]. The situation seems to be
92 complicated by the effect of temperature and surface moisture other than agar and nutrient
93 concentrations. Therefore, we introduced environmental pH as a new parameter and attempted to
94 clarify the growth condition requirements of *B. subtilis*.

95 Except for concentric colonies, the dominant cell type is often defined as either a motile cell or matrix

96 producer. First, colonies formed by swarming motile cells are formed under an agar concentration of
97 0.4–0.7%. These colonies are classified into two types according to the nutrient concentration: disk-
98 like (high nutrition)[34, 35] and dense branching morphology (DBM)-like (low nutrition)[36-39]. On the other
99 hand, the slowly expanding colonies dominated by matrix producers are formed on a solid medium
100 with an agar concentration of 0.7% or more. These colonies are also classified into two types, namely,
101 Eden cluster-like (high nutrition)[40-42] and diffusion-limited-aggregation (DLA)-like (low nutrition)[43-
102 46], depending on the nutrient concentration[44, 45]. In general, the classification is based on these five
103 types. A detailed examination revealed that a small number of motile cells were mixed even on the
104 surface of a hard medium with an agar concentration of 1%, which affected macroscopic colony
105 morphology and expansion rate[47]. Particularly, a crater-like pattern in which cells gather at the tip of
106 the colony is formed by only slightly lowering the environmental pH from the intracellular pH of 7.4.
107 This is due to chemotaxis toward nutrients, which is a phenomenon that does not occur during
108 swarming[27]. Chemotaxis is also observed in concentric colonies. Specifically, in the inner region after
109 the end of the migration phase, slow swimming migration of the cell population occurs because of
110 chemotaxis from the inside to the outside, and as a result, the ring tip becomes longer. The mechanism
111 of this phenomenon is the same as that for crater-like pattern formation. On the other hand, when the
112 agar concentration is low (0.5%), swift colony expansion via swarming is observed because the energy
113 required for migration is low due to the availability of abundant water on the surface of the medium.
114 However, under certain conditions, i.e., optimum pH of 7.4, the dominant cell types become matrix
115 producers rather than motile cells, and lacework-patterned colonies may be formed[23]. Thus, other than
116 concentric colonies, different stress parameters, such as environmental pH, influence the choice
117 between motile cells and matrix producers.
118 Here, we investigate the effect of environmental pH on cell-type selection and concentric *B. subtilis*
119 colony formation. By quantitative analysis of culture experiments, we clarify the range of
120 environmental pHs in which concentric colonies are formed, and the environmental pH dependence of

121 the temporal and spatial cycles within that range. Further, by combining the mathematical model of
122 cell-type regulation on the basis of the conventional gene regulatory network and analysis of its
123 mathematical properties, we propose a model for type regulation of cell population that changes
124 depending on the environment. Our proposed model provides a reasonable explanation for the
125 formation of concentric circular colonies and subsequent biofilm life cycle generation.

126 Results

127 Concentric colonies embody the biofilm life cycle

128 We prepared a medium with a high nutrient concentration and an intermediate agar concentration of
129 0.7% among the range of solid agar media (containing 0.2% or more agar), and inoculated *B. subtilis*
130 onto the center. When the plate was cultured at about 35°C, concentric colonies were formed on the
131 medium surface (Fig. 1). This is a simple model for biofilm life cycle generation, and its temporal and
132 spatial cycles embody that life cycle. We captured two-dimensional transmitted light images of this
133 colony using a scanner (Fig. 1a). The image data were converted to cell density distribution (Fig. 1b),
134 using which a 3D structure was reconstructed (Fig. 1c), and the cross-section was analyzed (Fig. 1d).
135 By performing such quantitative analyses in a time series, not only the two-dimensional cell density
136 (colony thickness) but also the dynamics of cell proliferation and migration were analyzed (Fig. 2).
137 The boundaries of colonies were identified at each time and the depth of each terrace was measured
138 (Fig. 2a, b). The concentric colonies of *B. subtilis* have distorted boundaries unlike those of *Proteus*
139 *mirabilis*. Therefore, the colony radius r was defined from area A of the inner area of the colony:
140 $r = \sqrt{A/\pi}$. Then, from the increase in the colony radius, the migration and growth phases of *B. subtilis*
141 biofilm, and their combined life cycle were observed (Fig. 2c).

142 Microscopic observation of phase switching in concentric colonies

143 Using phase-contrast microscopy, we investigated how the concentric colony formation phase

144 transition occurred, and how the cell state and its spatial distribution changed. First, the termination
145 process of the growth phase, in which matrix producers are dominant, begins with the appearance of
146 motile cells just before the colony boundary (Fig. 3a). There, motile cells continue to grow and form
147 ponds wherein cell swarming occurs. The surrounding cells are partially separated from each other by
148 autolysins[29, 30, 48, 49], and the pressure of proliferating motile cells is also applied, destroying many
149 points in the colony border area.

150 Among those destroyed points, the breakage starts at points on the outer side of the colony boundary,
151 and motile cells flow out from there to form branches (Fig. 3b, c, Supplementary Video S1). The
152 migration phase where motile cells are dominant is shown in Fig. 3d-f. In this phase, the formed
153 branches quickly expand outward because of swarming (Fig. 3d, Supplementary Video S2). Then, the
154 number of break points near the root increases, and the gap between branches is filled with outflow
155 cells from the inside (Fig. 3e, f, Supplementary Videos S3, S4). The end of the migration phase begins
156 when the branches stop growing (Fig. 3g). Immediately thereafter, the swarming area shrinks from the
157 tip of the branch toward the inner root (Fig. 3g-i). When there is no swarming region, the growth phase
158 begins. In the growth phase, the cells do not move and proliferate, and the cell density increases. The
159 cell density is considered to be measured by the cells themselves by the concentration of the secreted
160 quorum-sensing factor ComX[50-52]. When the concentration exceeds a certain threshold, motile cells
161 reappear, and transition to the migration phase occurs (Fig. 3a). This is one round of the life cycle of
162 *the B. subtilis* cell population.

163 Effect of environmental pH on periodically expanding colonies

164 The conditions for forming concentric colonies of *B. subtilis* have been investigated. Particularly,
165 under optimal conditions (incubation temperature around 35–37°C), concentric circular colonies are
166 formed only in an extremely narrow range of agar concentration of 0.65–0.68%, even if nutritional
167 conditions are suitable[21]. It can be inferred that other stress parameters, such as low temperature[19], are

168 necessary for the formation of concentric colonies. We investigated the effect of environmental pH as
169 a stress parameter. Conditions other than environmental pH were optimal, and the agar concentration
170 was set at an intermediate level of 0.7% (Fig. 4). First, in the neutral pH region, no periodically growing
171 colonies appeared. Matrix producers were the predominant cell type, and colonies grew by increasing
172 their volume via proliferation (Fig. 4a, b). As the environmental pH decreased, many, very-short
173 migration phases appeared around pH 6.8. Under the pH condition close to this transition point, the
174 variation in space was very strong, the periodicity was not clear, and the pattern was far from that of
175 concentric circles. When the pH decreased below 6.5, concentric circular colonies that expand
176 periodically were formed. When the pH was lower than 5.3, colony formation itself became unstable,
177 and the colony formation stopped halfway or no colonies were formed. Finally, below pH 5.1, colonies
178 were not always formed. In summary, the stable pH range for cyclic growth of colonies was 5.3–6.5.
179 Next, we investigated the properties of concentric colonies in this pH range. First, the circularity of
180 the ring was constant, although there was some variation in the pattern transition region near the neutral
181 pH (Fig. 4c). The spatial period (width of the swarm ring) seemed to increase monotonically as pH
182 decreased (Fig. 4d). Specifically, in the pattern transition region (pH 6.0–6.5), the spatial period
183 sharply increased with decreasing pH, and then it had a substantially constant period in the range of
184 pH 5.3–6.0.
185 To clarify how these differences in colony morphology were produced, we examined the periods of
186 each growth phase and migration phase (Fig. 4e). We found that while the total time period was almost
187 constant, the growth phase duration decreased as the pH decreased; conversely, the duration of the
188 migration phase increased. Specifically, the finer spatial patterns reflected shorter migration periods,
189 while the total length of the life cycle of the cell population seemed homeostatic.

190 Environment-dependent regulation of cells and cell populations

191 We investigated the mechanism of control of the two different states of the cell population (migration

192 and growth phases). Cell population control should be understood on the basis of cell-level regulation
193 in response to environmental conditions The regulation between the two cell types, motile cells and
194 matrix producers, is well studied, particularly the switch between planktonic and biofilm states[24, 53-56].
195 The two cell types are designed to have mutually exclusive gene expression states. We created a simple
196 mathematical model to investigate cellular state dynamics (Fig. 5a). In this model, cell states can be
197 described according to four group variables by grouping coordinated genes and their products: (1) S :
198 A group represented by Spo0A~P, which also includes phosphorelay of Spo0F, Spo0B, and Spo0A;
199 (2) H: SigH; (3) A: AbrB; (4) C: A group represented by ComK, driven by the ComX-ComP-
200 ComA pathway.

201 The output of this control system is the cell type. In this case, it is a matrix producer when S is
202 high and a motile cell when S is low. Sporulation is initiated when S is continuously very high.
203 However, predominant sporulation occurs at a nutrient-depletion stage much later than colonization.
204 Therefore, it is not necessary to consider sporulation here. On the other hand, the inputs of the cell
205 state control system include external environmental conditions and auto-inducing signals that represent
206 cell density. There are various environmental conditions. For example, poor nutritional conditions may
207 be input to activate S, but we considered the formation of periodic growth colonies, and the initial
208 nutrient concentration was sufficiently high. Therefore, the nutritional conditions were constant and
209 sufficient at the time of colony formation. As an auto-inducing signal related to cell-type control, a
210 small peptide ComX is secreted by *B. subtilis* cells[50-52]. In the following equation, its concentration is
211 denoted as X, which is an input from C to the cell-type regulation system[50, 51, 57]. The input mode of
212 environmental pH is of significant interest at this stage. According to previously performed studies,
213 H or A is the candidate input point for external pH in the current model[58, 59].

214 Here, we considered the most minimal and smooth dynamic model of these four variables
215 ("Methods"). The curve of the set of equilibrium points can be divided into two types: with respect to
216 the increase and decrease in X, the variable that represents the cell state (for example, S) is

217 monotonic and non-monotonic (Fig. 5b, c)[60]. In the latter case, the curve is an S-shaped curve with
218 two turning points. Specifically, there are two cases where cell-type control is either not hysteretic (Fig.
219 5b) or hysteretic (Fig. 5c), considering the increase/decrease in the cell density signal X. The latter
220 hysteretic control is necessary for biofilm life cycle generation and concentric colony formation. When
221 there is hysteresis in the choice of cell state for increasing and decreasing X, a life cycle is created
222 for the cell population as follows. Migration phase: the cell density information X at the growth front
223 decreases as the cell population disperses in the motility state, and when it falls below a certain
224 threshold X_1, the cell population switches to the matrix-producing state. Growth phase: as the cell
225 population grows and matures in the matrix-producing state, X increases, and when it exceeds a
226 certain threshold $X_2 \left(> X_1\right)$, the cell population switches to the motility state again.

227 AbrB is upregulated and SigH is suppressed as the environmental pH decreases in the weakly acidic
228 region of interest[58, 59]. These two are potential candidates for inputting environmental pH information.
229 It is not easy to determine which of these two elements, which suppress each other in the regulatory
230 network, is upstream for inputting external pH information. According to the detailed mathematical
231 analysis of the equilibrium state of this model, a situation in which hysteresis occurs with a decrease
232 in environmental pH and concentric colonies are formed can be realized only when AbrB is the input
233 point for pH (Fig. 5a, d; "Methods")[60] . Therefore, we proposed a model of cell-type regulation using
234 AbrB as the input point for environmental pH information (Fig. 5a). On the basis of this cell-type
235 regulation model, the generation mechanism of the life cycle of the cell population in the parameter
236 range for hysteretic control could be explained (Fig. 5c), and the dependence on environmental
237 conditions could be understood.

238 Discussion

239 We have presented a possible mechanism of formation of *B. subtilis* concentric colonies that expand
240 periodically and embody the life cycle of the cell population. By performing culturing experiments

241 and their quantitative analysis, the dynamics of colony growth and its environmental pH dependence
242 were clarified from a multilevel perspective—from the cell level to the macroscopic morphological
243 level. We sought to understand patten formation under the assumption that the predominant cell type
244 switches between motile cells and immotile cells, such as matrix producers. Based on the accumulation
245 of molecular biology research to date, the outline of the gene regulatory network responsible for the
246 regulation between these two cell types of *B. subtilis* has been established. We proposed a model of
247 cell-type regulation by environmental conditions and cell density by combining concentric colony
248 culture experiments under different environmental pH conditions. The mathematical properties of the
249 minimal smooth model describing the dynamics also suggested the input location of environmental
250 pH in the cell-type regulation system. The obtained model should be a general control mechanism that
251 selects an appropriate cell population structure depending on the situation. Particularly, the S-shaped
252 curve of the set of equilibrium points obtained by this mathematical model analysis makes it possible
253 to understand the hysteretic control of the cell population that forms concentric colonies, and
254 subsequently, the migration cycle generation mechanism.

255 In the cell population migration cycle, phase switches are dependent on cell density. We investigated
256 the switching mechanism and found that the migration cycle was stably modulated via hysteretic
257 control of cell type. Further, the effect of environmental conditions can be predicted. At present,
258 however, environmental changes and cell type control were investigated via concentric circle colony
259 formation experiments under environmental pH (and only neutral to acidic) conditions. In the future,
260 we plan to elucidate how *B. subtilis* cells collectively cope with fluctuations in a large range of pH,
261 particularly via the study of the responses at high pH. Moreover, to predict the response to changes in
262 other environmental conditions, such as nutrient concentration, temperature, and oxygen concentration,
263 it is necessary to understand a wider gene regulatory network. Nevertheless, the conditions for biofilm
264 life cycle generation can be better organized as per the presence or absence of hysteresis. Of note, this
265 classification will probably be applicable to biofilm life cycle studies focusing on other microbial

species.

A morphological diagram was created for understanding the colony morphology of *B. subtilis* in the 1990s[34, 61], in which one of the five colonies was formed depending on the two parameters, nutrient concentration and agar concentration, in the medium. These five colonies are called Eden cluster-like[40-42], DLA-like[43-46, 62, 63], concentric ring-like, disk-like[34, 35], and DBM-like[36-39], respectively. The concept of cell type was not established at the time, but it is now well-understood, and the colony pattern can be explained as follows. The dominant cell type is immotile cells, such as matrix producers, in Eden cluster-like and DLA-like colonies; disk-like and DBM-like colonies have motile cells as the predominant cell type. Finally, in the concentric ring-like colony, the dominant cell type switches between motile cells and immotile cells. Thus, among the five patterns, concentric colonies had multiple dominant cell types, which created unsolved problems. The mechanism of pattern formation was unknown, and it was not understood or reproduced by a mathematical model[64]. Our proposed model for cell-type regulation has presented one possible mechanism for this problem.

Furthermore, the concentric colonies presented uncertainties, even with respect to the formation conditions, such as an extremely narrow agar concentration range[21] and the dependence on culture temperature[19]. Apparently, parameters other than agar and nutrient concentrations were likely involved in the formation of concentric colonies. In other words, introducing some kind of a stress parameter is effective for concentric pattern formation. We obtained the conditions to stably form concentric colonies by introducing environmental pH. By drawing the morphology diagram in a three-parameter space, it is possible to understand the entire cell population morphology correctly and in detail. By incorporating our cell-type regulation model into a multilevel morphogenesis model, we expect to obtain a simulation model that accurately predicts the growth of multicellular systems with non-uniform cell state distribution.

Robust biofilms and other complex cell populations of microorganisms are social structures involved in the organization of diverse cell types. Therefore, understanding the mode of state regulation of each

291 cell should be the first key to understanding and controlling the behavior of the cell population as a
292 whole. Therefore, higher-order structures of cell populations are self-organized in a trans-hierarchical
293 manner: from gene-level and cell-level control to microscopic structures, macroscopic morphology
294 and function of cell populations, and interaction with the surrounding environment. Thus, the
295 construction of multilevel models for controlling the state of cell populations will strongly advance
296 the research on various multicellular societies.

297 Methods

298 Experimental methods

299 *B. subtilis* wild-type strain OG-01 (JCM32485) was used[44, 65]. A very small quantity of bacteria
300 (endospores) was incubated overnight (10–16 h) in 5 mL of Luria–Bertani liquid growth medium (LB
301 Broth Base (Lennox L Broth Base), Gibco BRL Life Technologies, cat. no. 12780-052) at 35°C with
302 shaking at 140 rpm. For inoculation on solid agar media, this final pellet was diluted with the buffer
303 to an OD_{600} of 0.5.

304 A solution of 86 mM NaCl and 29 mM K_2HPO_4 was prepared. As a nutrient, 20 g L^{-1} peptone (Bacto
305 Peptone, BD Biosciences, cat. no. 211677) was added to the solution, and the pH was then adjusted to
306 a designated value by adding 6 M HCl, and 0.7% agar (Bacto Agar, BD Biosciences, cat. no. 214010)
307 was added to the above liquid nutrient medium. After autoclaving at 121°C for 15 min, 20 mL of the
308 solution was poured into each plastic Petri dish. The dishes were maintained at room temperature
309 overnight and dried at 50°C for 90 min.

310 The pre-cultured bacterial suspension was inoculated using a sterilized needle at the center of the
311 prepared solid medium surface. The dishes were incubated in a humidified box at 35°C for the
312 designated time. Macroscopic colony-transmitted light images were obtained using a flat head scanner
313 (GT-X980, Epson). Cell or cell cluster level morphology was observed by phase-contrast microscopy
314 using an inverted microscope (IX83, Olympus) with a camera (DP80, Olympus).

Mathematical model of dynamic cell-type regulation.

To describe the dynamics of cell-type control (Fig. 5a), we consider the following minimal smooth model:

$$\begin{aligned} \frac{dS}{dt} &= \frac{c_S H}{a_S + b_S C} - d_S S \\ \frac{dH}{dt} &= \frac{c_H}{a_A + b_A A} - d_H H \\ \frac{dA}{dt} &= \frac{c_A}{a_A + b_A S} - d_A A \\ \frac{dC}{dt} &= c_C X A - d_C C \end{aligned} \tag{1}$$

where $a_*, b_*, c_*, d_* \quad (* = S, H, A, C)$ are positive constants. There are two cases where cell-type control is non-hysteretic (Fig. 5b) and hysteretic (Fig. 5c), regarding the increase/decrease in the cell density signal *X*. We set a parameter indicating the rate at which AbrB is activated from outside the model system of cell-type regulation (equation (1); Fig. 5a) as follows:

$$I_A = \frac{b_H}{a_H} \times \frac{c_A / a_A}{d_A} \tag{2}$$

Similarly, we define the rate at which Spo0A~P and SigH are activated from outside the model system as

$$I_{SH} = \frac{b_A}{a_A} \times \frac{c_S / a_S}{d_S} \times \frac{c_H / a_H}{d_H} \tag{3}$$

Particularly, the external activation rate of AbrB $I_A = I_{\mathrm{AbrB}}$ is the horizontal axis in Fig. 5d. Thus, the following can be proved[60]: There exists $I_{SH}^* > 0$ such that

1. If $I_{SH} \le I_{SH}^*$, then the steady states are anhysteretic (Fig. 5b).
2. If $I_{SH} > I_{SH}^*$, then there exists $1 < I_{A,L} < I_{A,U}$ such that

331 **(i)** If $0 < I_A \leq I_{A,L}$, then the steady states are anhysteretic (Fig. 5b).

332 **(ii)** If $I_{A,L} < I_A < I_{A,U}$, then the steady states are hysteretic (Fig. 5c).

333 **(iii)** If $I_{A,U} \leq I_A$, then the steady states are anhysteretic (Fig. 5b).

334 Case 2 above (the external activation of Spo0A~P and SigH is larger than the threshold $I_{SH} > I_{SH}^*$)
335 shows the situation in Fig. 5d, and it is also in agreement with the experimental results, suggesting that
336 $I_A = I_{\mathrm{AbrB}}$ plays the role of a parameter corresponding to the environmental pH reduction. Note the
337 mathematical feature that at least AbrB must be actively involved to reproduce the pH dependence of
338 cell type control[60]. In the past literature, SigH or AbrB, especially SigH, was a candidate[58, 59], but at
339 least SigH alone does not show the observed pH dependence of cell type control in the mathematical
340 model.
341

342 # Acknowledgments

343 This work was supported by JSPS KAKENHI, Grant Number 19K03645 (S.T.), and MEXT
344 KAKENHI, Grant Number 17H06327 (S.T.).

345 # Author contributions

346 S.T., M.N. and W.S. conceived the study. S.T. and M.N. designed and performed the experiments, and
347 analyzed the data. S.T. and M.N. constructed the mathematical model. S.T., M.N. and I.T. analyzed
348 the model. S.T. and M.N. wrote the manuscript. All authors reviewed the manuscript.

349 # References

350 1. Stoodley P, Sauer K, Davies DG, Costerton JW. Biofilms as Complex Differentiated
351 Communities. *Annu Rev Microbiol* **56**, 187-209 (2002).
352

2. Donlan RM. Biofilms: microbial life on surfaces. *Emerg Infect Dis* **8**, 881-890 (2002).

3. Hall-Stoodley L, Costerton JW, Stoodley P. Bacterial biofilms: from the natural environment to infectious diseases. *Nat Rev Microbiol* **2**, 95-108 (2004).

4. Branda SS, Vik Å, Friedman L, Kolter R. Biofilms: the matrix revisited. *Trends Microbiol* **13**, 20-26 (2005).

5. Kobayashi K, Iwano M. BslA(YuaB) forms a hydrophobic layer on the surface of *Bacillus subtilis* biofilms. *Mol Microbiol* **85**, 51-66 (2012).

6. Vlamakis H, Chai Y, Beauregard P, Losick R, Kolter R. Sticking together: building a biofilm the *Bacillus subtilis* way. *Nat Rev Microbiol* **11**, 157-168 (2013).

7. Hobley L, Harkins C, MacPhee CE, Stanley-Wall NR. Giving structure to the biofilm matrix: an overview of individual strategies and emerging common themes. *FEMS Microbiol Rev* **39**, 649-669 (2015).

8. Flemming H-C, Wingender J, Szewzyk U, Steinberg P, Rice SA, Kjelleberg S. Biofilms: an emergent form of bacterial life. *Nature Reviews Microbiology* **14**, 563-575 (2016).

9. Gilbert P, Das J, Foley I. Biofilm susceptibility to antimicrobials. *Adv Dent Res* **11**, 160-167 (1997).

10. Mah TF, O'Toole GA. Mechanisms of biofilm resistance to antimicrobial agents. *Trends Microbiol* **9**, 34-39 (2001).

11. Hall CW, Mah T-F. Molecular mechanisms of biofilm-based antibiotic resistance and tolerance in pathogenic bacteria. *FEMS Microbiol Rev* **41**, 276-301 (2017).

12. Kostakioti M, Hadjifrangiskou M, Hultgren SJ. Bacterial biofilms: development, dispersal, and therapeutic strategies in the dawn of the postantibiotic era. *Cold Spring Harb Perspect Med* **3**, a010306-a010306 (2013).

13. Algburi A, Comito N, Kashtanov D, Dicks LMT, Chikindas ML. Control of Biofilm Formation:

Antibiotics and Beyond. *Appl Environ Microbiol* **83**, e02508-02516 (2017).

14. Galié S, García-Gutiérrez C, Miguélez EM, Villar CJ, Lombó F. Biofilms in the Food Industry: Health Aspects and Control Methods. *Front Microbiol* **9**, (2018).

15. Bisset KA. The zonation phenomenon and structure of the swarm colony in *Proteus mirabilis*. *J Med Microbiol* **6**, 429-433 (1973).

16. Rauprich O, Matsushita M, Weijer CJ, Siegert F, Esipov SE, Shapiro JA. Periodic phenomena in *Proteus mirabilis* swarm colony development. *J Bacteriol* **178**, 6525-6538 (1996).

17. Matsuyama T, Takagi Y, Nakagawa Y, Itoh H, Wakita J, Matsushita M. Dynamic Aspects of the Structured Cell Population in a Swarming Colony of *Proteus mirabilis*. *J Bacteriol* **182**, 385-393 (2000).

18. Yamazaki Y*, et al.* Periodic growth of bacterial colonies. *Physica D: Nonlinear Phenomena* **205**, 136-153 (2005).

19. Fujikawa H. Periodic growth of *Bacillus subtilis* colonies on agar plates. *Physica A: Statistical Mechanics and its Applications* **189**, 15-21 (1992).

20. Itoh H, Wakita J-i, Matsuyama T, Matsushita M. Periodic pattern formation of bacterial colonies. *J Phys Soc Japan* **68**, 1436-1443 (1999).

21. Wakita J, Shimada H, Itoh H, Matsuyama T, Matsushita M. Periodic colony formation by bacterial species *Bacillus subtilis*. *J Phys Soc Japan* **70**, 911-919 (2001).

22. Shimada H*, et al.* Dependence of local cell density on concentric ring colony formation by bacterial species *Bacillus subtilis*. *J Phys Soc Japan* **73**, 1082-1089 (2004).

23. Tasaki S, Nakayama M, Shoji W. Morphologies of *Bacillus subtilis* communities responding to environmental variation. *Dev Growth Differ* **59**, 369-378 (2017).

24. López D, Vlamakis H, Kolter R. Generation of multiple cell types in *Bacillus subtilis*. *FEMS Microbiol Rev* **33**, 152-163 (2009).

423
424 25. Kearns DB, Losick R. Swarming motility in undomesticated *Bacillus subtilis*. *Mol Microbiol*
425 **49**, 581-590 (2003).
426
427 26. Kearns DB, Chu F, Rudner R, Losick R. Genes governing swarming in *Bacillus subtilis* and
428 evidence for a phase variation mechanism controlling surface motility. *Mol Microbiol* **52**, 357-
429 369 (2004).
430
431 27. Kearns DB. A field guide to bacterial swarming motility. *Nat Rev Microbiol* **8**, 634-644 (2010).
432
433 28. Marvasi M, Visscher PT, Casillas Martinez L. Exopolymeric substances (EPS) from *Bacillus*
434 *subtilis*: polymers and genes encoding their synthesis. *FEMS Microbiol Lett* **313**, 1-9 (2010).
435
436 29. Smith TJ, Blackman SA, Foster SJ. Autolysins of *Bacillus subtilis*: multiple enzymes with
437 multiple functions. *Microbiology* **146**, 249-262 (2000).
438
439 30. Chai Y, Norman T, Kolter R, Losick R. An epigenetic switch governing daughter cell separation
440 in *Bacillus subtilis*. *Genes Dev* **24**, 754-765 (2010).
441
442 31. Nakano MM, Magnuson R, Myers A, Curry J, Grossman AD, Zuber P. *srfA* is an operon
443 required for surfactin production, competence development, and efficient sporulation in
444 *Bacillus subtilis*. *J Bacteriol* **173**, 1770-1778 (1991).
445
446 32. Nakano MM, Xia LA, Zuber P. Transcription initiation region of the *srfA* operon, which is
447 controlled by the *comP-comA* signal transduction system in *Bacillus subtilis*. *J Bacteriol* **173**,
448 5487-5493 (1991).
449
450 33. van Gestel J, Vlamakis H, Kolter R. From cell differentiation to cell collectives: *Bacillus*
451 *subtilis* uses division of labor to migrate. *PLoS Biol* **13**, e1002141 (2015).
452
453 34. Wakita J, Komatsu K, Nakahara A, Matsuyama T, Matsushita M. Experimental investigation
454 on the validity of population dynamics approach to bacterial colony formation. *J Phys Soc*
455 *Japan* **63**, 1205-1211 (1994).
456
457 35. Wakita J, Kuninaka H, Matsuyama T, Matsushita M. Size distribution of bacterial cells in

homogeneously spreading disk-like colonies by *Bacillus subtilis*. *J Phys Soc Japan* **79**, 094002 (2010).

36. Grier D, Ben-Jacob E, Clarke R, Sander LM. Morphology and microstructure in electrochemical deposition of zinc. *Phys Rev Lett* **56**, 1264-1267 (1986).

37. Sawada Y, Dougherty A, Gollub JP. Dendritic and fractal patterns in electrolytic metal deposits. *Phys Rev Lett* **56**, 1260-1263 (1986).

38. Ben-Jacob E, Garik P. The formation of patterns in non-equilibrium growth. *Nature* **343**, 523-530 (1990).

39. Wakita J, Ràfols I, Itoh H, Matsuyama T, Matsushita M. Experimental investigation on the formation of dense-branching-morphology-like colonies in bacteria. *J Phys Soc Japan* **67**, 3630-3636 (1998).

40. Eden M. A two-dimensional growth process. In: *Proceedings of the Fourth Berkeley Symposium on Mathematical Statistics and Probability, Volume 4: Contributions to Biology and Problems of Medicine*). University of California Press (1961).

41. Vicsek T, Cserző M, Horváth VK. Self-affine growth of bacterial colonies. *Physica A: Statistical Mechanics and its Applications* **167**, 315-321 (1990).

42. Wakita J, Itoh H, Matsuyama T, Matsushita M. Self-affinity for the growing interface of bacterial colonies. *J Phys Soc Japan* **66**, 67-72 (1997).

43. Witten TA, Sander LM. Diffusion-limited aggregation, a kinetic critical phenomenon. *Phys Rev Lett* **47**, 1400-1403 (1981).

44. Fujikawa H, Matsushita M. Fractal growth of *Bacillus subtilis* on agar plates. *J Phys Soc Japan* **58**, 3875-3878 (1989).

45. Matsushita M, Fujikawa H. Diffusion-limited growth in bacterial colony formation. *Physica A: Statistical Mechanics and its Applications* **168**, 498-506 (1990).

493 46. Fujikawa H, Matushita M. Bacterial fractal growth in the concentration field of nutrient. *J Phys*
494 *Soc Japan* **60**, 88-94 (1991).
495
496 47. Tasaki S, Nakayama M, Shoji W. Self-organization of bacterial communities against
497 environmental pH variation: Controlled chemotactic motility arranges cell population
498 structures in biofilms. *PLoS One* **12**, e0173195 (2017).
499
500 48. Blackman SA, Smith TJ, Foster SJ. The role of autolysins during vegetative growth of *Bacillus*
501 *subtilis* 168. *Microbiology* **144**, 73-82 (1998).
502
503 49. Vollmer W, Joris B, Charlier P, Foster S. Bacterial peptidoglycan (murein) hydrolases. *FEMS*
504 *Microbiol Rev* **32**, 259-286 (2008).
505
506 50. Magnuson R, Solomon J, Grossman AD. Biochemical and genetic characterization of a
507 competence pheromone from *B. subtilis*. *Cell* **77**, 207-216 (1994).
508
509 51. Ansaldi M, Marolt D, Stebe T, Mandic-Mulec I, Dubnau D. Specific activation of the *Bacillus*
510 quorum-sensing systems by isoprenylated pheromone variants. *Mol Microbiol* **44**, 1561-1573
511 (2002).
512
513 52. Okada M*, et al.* Structure of the *Bacillus subtilis* quorum-sensing peptide pheromone ComX.
514 *Nat Chem Biol* **1**, 23-24 (2005).
515
516 53. Kearns DB, Losick R. Cell population heterogeneity during growth of *Bacillus subtilis*. *Genes*
517 *Dev* **19**, 3083-3094 (2005).
518
519 54. Kobayashi K. Gradual activation of the response regulator DegU controls serial expression of
520 genes for flagellum formation and biofilm formation in *Bacillus subtilis*. *Mol Microbiol* **66**,
521 395-409 (2007).
522
523 55. Chai Y, Chu F, Kolter R, Losick R. Bistability and biofilm formation in *Bacillus subtilis*. *Mol*
524 *Microbiol* **67**, 254-263 (2008).
525
526 56. Cairns LS, Hobley L, Stanley-Wall NR. Biofilm formation by *Bacillus subtilis*: new insights
527 into regulatory strategies and assembly mechanisms. *Mol Microbiol* **93**, 587-598 (2014).

57. Grossman AD, Losick R. Extracellular control of spore formation in *Bacillus subtilis*. *Proc Natl Acad Sci USA* **85**, 4369-4373 (1988).

58. Cosby WM, Zuber P. Regulation of *Bacillus subtilis* σH (Spo0H) and AbrB in response to changes in external pH. *J Bacteriol* **179**, 6778-6787 (1997).

59. Wilks JC*, et al.* Acid and base stress and transcriptomic responses in *Bacillus subtilis*. *Appl Environ Microbiol* **75**, 981-990 (2009).

60. Tasaki S, Nakayama M, Takagi I, Wakita J, Shoji W. Necessary and sufficient condition for hysteresis in the mathematical model of the cell type regulation of *Bacillus subtilis*. *arXiv*, 2009.06524 (2020).

61. Ohgiwari M, Matsushita M, Matsuyama T. Morphological changes in growth phenomena of bacterial colony patterns. *J Phys Soc Japan* **61**, 816-822 (1992).

62. Ben-Jacob E, Shmueli H, Shochet O, Tenenbaum A. Adaptive self-organization during growth of bacterial colonies. *Physica A: Statistical Mechanics and its Applications* **187**, 378-424 (1992).

63. Ben-Jacob E, Schochet O, Tenenbaum A, Cohen I, Czirok A, Vicsek T. Generic modelling of cooperative growth patterns in bacterial colonies. *Nature* **368**, 46-49 (1994).

64. Mimura M, Sakaguchi H, Matsushita M. Reaction–diffusion modelling of bacterial colony patterns. *Physica A: Statistical Mechanics and its Applications* **282**, 283-303 (2000).

65. Matsuyama T, Matsushita M. Comments on 'Classification and genetic characterization of pattern-forming *Bacilli*' *Mol Microbiol* (1998) 27: 687–703. *Mol Microbiol* **31**, 1278-1279 (1999).

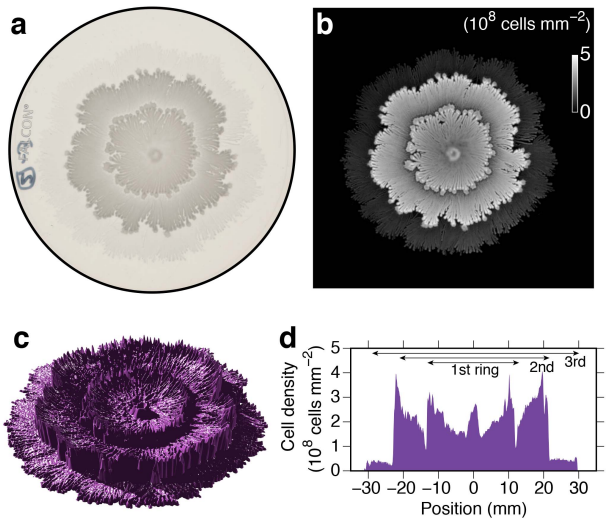

Fig. 1 Concentric ring-like colony embodies the life cycle. a Raw image of transmitted light obtained by a flat scanner. The center is the inoculation point. The diameter of the dish is 88 mm. **b** Two-dimensional cell density. **c** Three-dimensional reconstruction of the colony. **d** Cross-sectional view.

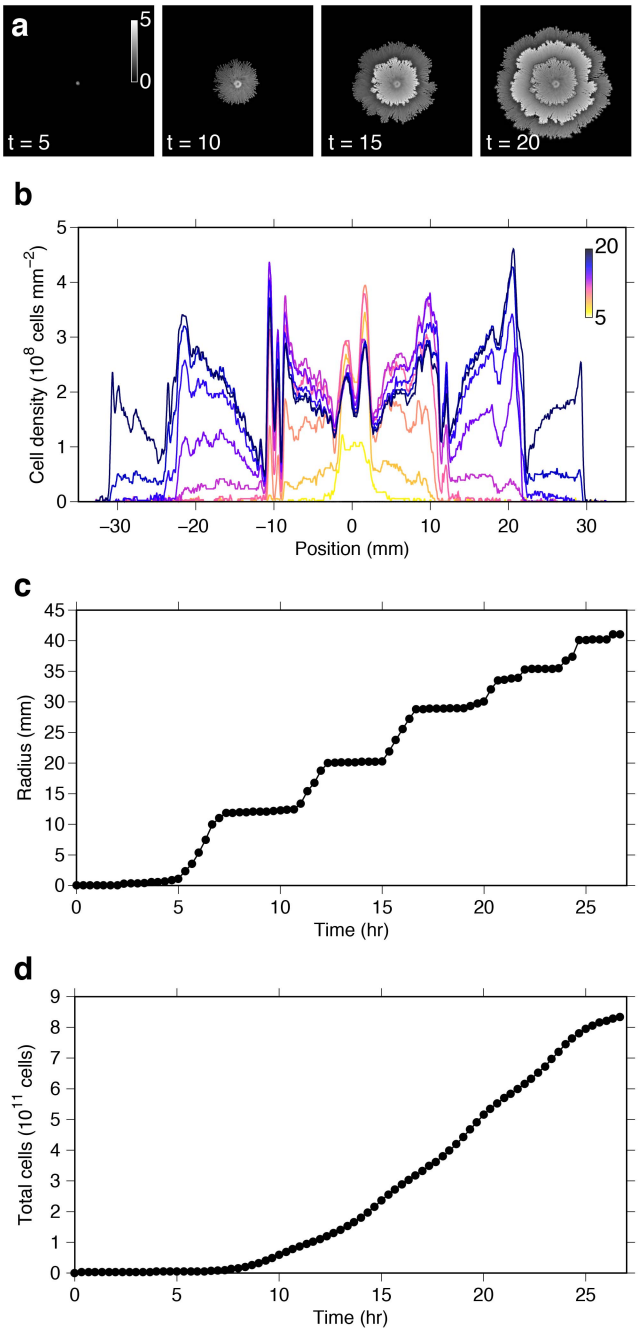

Fig. 2 Growth dynamics of concentric ring-like colony. a Two-dimensional cell density. Color bar, cell density (10^8 cells mm^{-2}). Incubation time, 5, 10, 15, and 20 h after inoculation. **b** Cross-section cell density. The center is the inoculation point. **c** Increasing colony radius. **d** Increasing total number of cells.

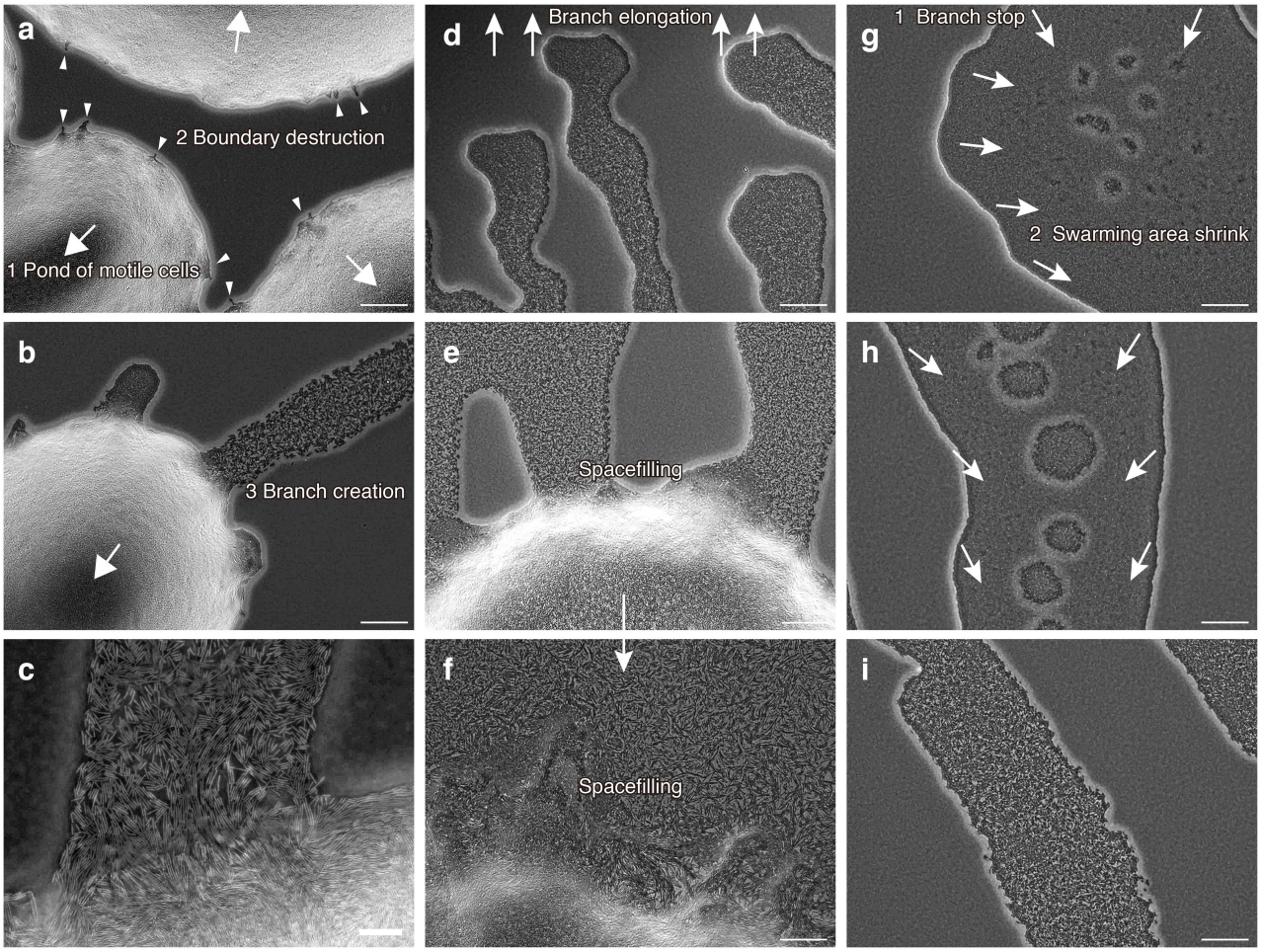

Fig. 3 Microscopic images of phase transition during colony expansion. a-c Transition from the growth phase to the migration phase. Motile cells appear slightly inside colony boundaries (large arrows in **a** and **b**). The number of motile cells increased to form bacterial ponds where cells organize to undergo swarming collective motion. The motile cells then destroy the boundary walls (small triangles in **a**). Cells flow out from some of the outermost destruction points on the colony boundaries to create rapidly expanding branches (**b** and **c**). **d-f** The migration phase. Numerous dense branches grow outward (**d**). Gradual collapse of the colony boundaries at the roots of branches, and the space around the roots is filled with the outflowing cells (**e** and **f**). **g-i** Transition from the migration phase to the growth phase. First, the branches stop growing (**g**). Then, the swarming regions composed of motile cells (small bubble-like regions in **g** and **h**; whole branch region in **i**) shrink from the outside to the inside of the colony (**g**, **h** to **i**; **g** is the outermost boundary, **i** is the innermost). Scale bars, 100 μm (except for **c**), 10 μm (**c**).

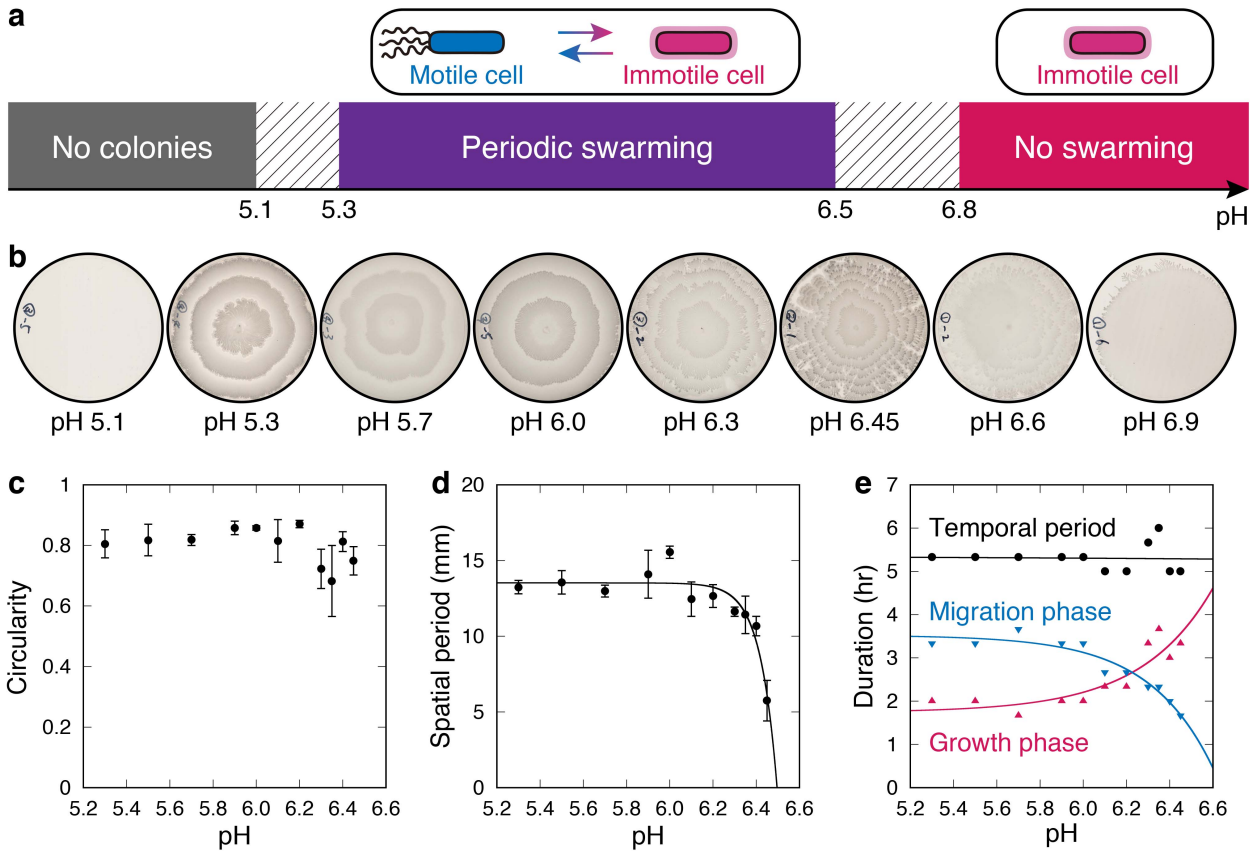

Fig. 4 Effect of environmental pH on periodically expanding colonies. a Environmental pH conditions for forming periodically expanding colonies. **b** Colonies under different environmental pH conditions. **c** Circularity of colony ring (defined by circularity of second ring). **d** Spatial period (width of terrace). **e** Time period: growth phase, migration phase, and total period. Data represent mean ± s.d., $n = 6$ (**c** and **d**). All fitting curves are exponential plus constant (**d** and **e**).

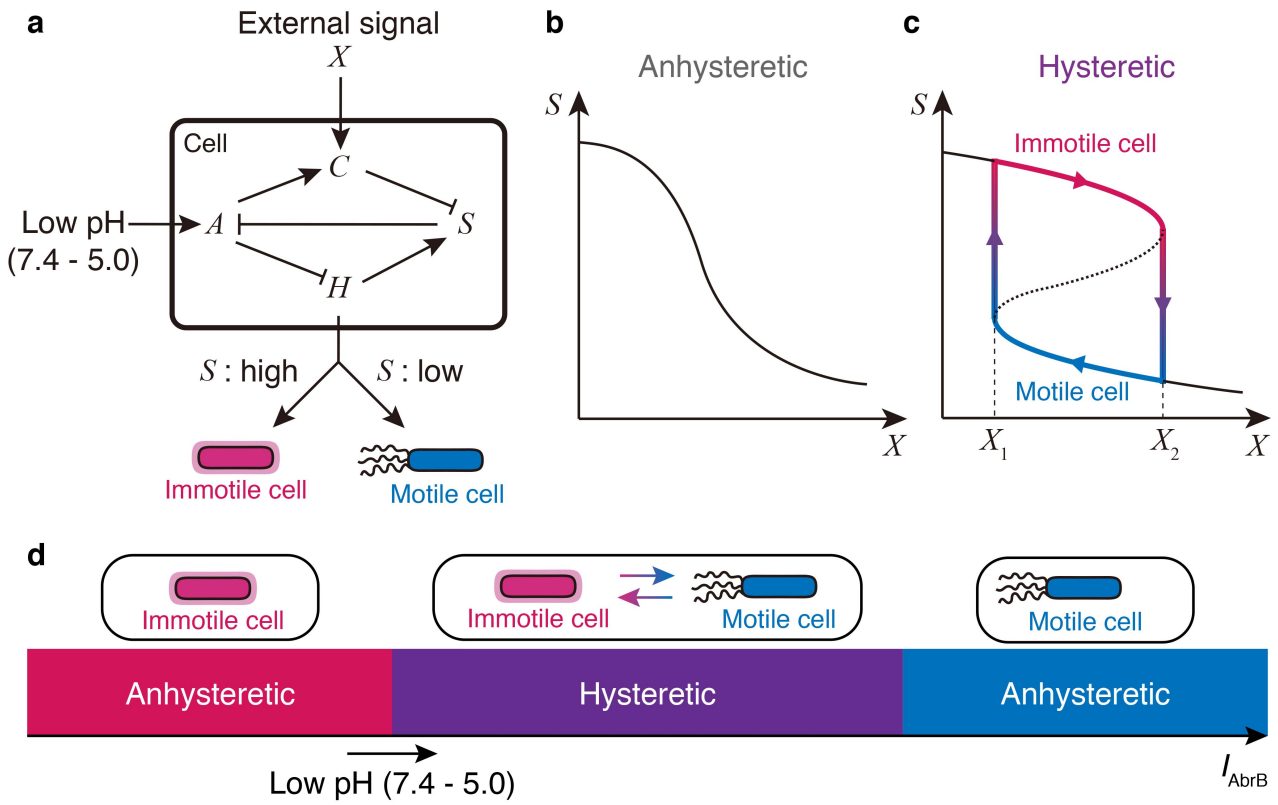

588 **Fig. 5 A model for the response of cells and cell populations to environmental pH. a** A model for
589 cell-type selection for environmental pH and cell density. **b, c** Two types of cell-type controls.
590 Anhysteretic (**b**) and hysteretic (**c**). **d** A model for cell population-type selection. The horizontal axis
591 (I_{AbrB}) is a parameter indicating the external activation rate of AbrB (see "Methods").

592

593